Earth and Planetary Science Letters 409 (2015) 225–231

Contents lists available at ScienceDirect

Earth and Planetary Science Letters

www.elsevier.com/locate/epsl

Refertilization-driven destabilization of subcontinental mantle and the importance of initial lithospheric thickness for the fate of continents

J.P. Zheng [a,*], C.-T.A. Lee [b,*], J.G. Lu [a], J.H. Zhao [a], Y.B. Wu [a], B. Xia [a], X.Y. Li [a], J.F. Zhang [a], Y.S. Liu [a]

[a] State Key Lab of Geological Processes and Mineral Resources, China University of Geosciences, Wuhan 430074, China
[b] Department of Earth Science, Rice University, 6100 Main St. Houston, TX 77005, United States

ARTICLE INFO

Article history:
Received 17 June 2014
Received in revised form 12 October 2014
Accepted 26 October 2014
Available online xxxx
Editor: Y. Ricard

Keywords:
continental destabilization
lithospheric initial thickness
refertilization
peridotite xenolith

ABSTRACT

Continents are underlain by thick, cold thermal boundary layers. Thermal contraction should render these boundary layers negatively buoyant and unstable; this is why old, cold oceanic lithospheres subduct. However, the ancient lithospheric roots of many continents appear to have existed for billions of years. In the common view, this preservation is due to the fact that the thermal boundary layers are compositionally distinct from the ambient mantle in that they are highly melt-depleted and dehydrated; the former provides positive buoyancy and the latter provides strength. Here, we show using mantle xenoliths that the Precambrian South China Block originally was underlain by highly depleted mantle, but has been refertilized via silicate melts generated from the asthenosphere. It is now more fertile than the ambient convecting mantle and is intrinsically denser by more than 1.5%. Achieving sufficient melt generation for refertilization is only possible if the lithosphere is thin enough to provide "headspace" for decompression melting. Thus, continental boundary layers thinner than the maximum depth of melting should experience refertilization, whereas thicker continents would altogether suppress melting and hence the potential for refertilization. We propose that refertilization, once initiated, will destabilize the base of the continent; this in turn will increase the amount of "headspace" and promote further refertilization, resulting in a positive feedback that could culminate in lithospheric destruction. By contrast, continents that are thick enough may not experience significant refertilization. This suggests that initial lithospheric thickness, as well as lithospheric composition, may be important for defining the fate of continents.

1. Introduction

The longevity of cratons is generally attributed to the highly melt-depleted lithospheric mantle that underlies the crust, providing a compositional buoyancy that compensates for the thermal contraction associated with the cooler thermal state of lithospheric mantle compared to the ambient convecting mantle (Jordan, 1978; Kelly et al., 2003). Such high degrees of melt-depletion requires unusually high temperatures, probably only achieved during the Archean and early Proterozoic when the mantle potential temperature was higher (Griffin et al., 2009; Herzberg and Rudnick, 2012). Although this might imply that all continental lithospheres formed during the Archean and early Proterozoic were highly melt-depleted and hence, destined for survival, there are some Archean to Proterozoic continental blocks, such as the North China Craton (Fig. 1a, Data Repository), the South China Block (e.g., Xu et al., 1998, 2002; Zheng et al., 2004; Liu et al., 2012a, 2012b; Lu et al., 2013), the North Atlantic Craton (Wittig et al., 2010; Hughes et al., 2014) and the Wyoming Craton (Carlson et al., 2004; Kusky et al., 2014), which have undergone significant Phanerozoic destruction. Why are these particular regions currently being destabilized, whereas other cratons have remained quiescent? Answering these questions is critical to understanding whether the present age distribution of continents reflects the tempo of continent formation or, instead, represents only what is left after destruction. The purpose of this study is to evaluate whether unstable continents are unstable because they do not have the necessary compositional characteristics for longevity or if additional factors must also be considered. To better understand how cratons are destabilized, we investigated the compositional and thermal structure of the lithospheric mantle beneath the South China Block.

* Corresponding authors. Tel.: +86 27 6788 3001; fax: +86 27 6788 3002 (J.P. Zheng), Tel.: +1 281 250 3606 (C.-T.A. Lee).
E-mail addresses: jpzheng@cug.edu.cn (J.P. Zheng), ctlee@rice.edu (C.-T.A. Lee).

http://dx.doi.org/10.1016/j.epsl.2014.10.042
0012-821X/

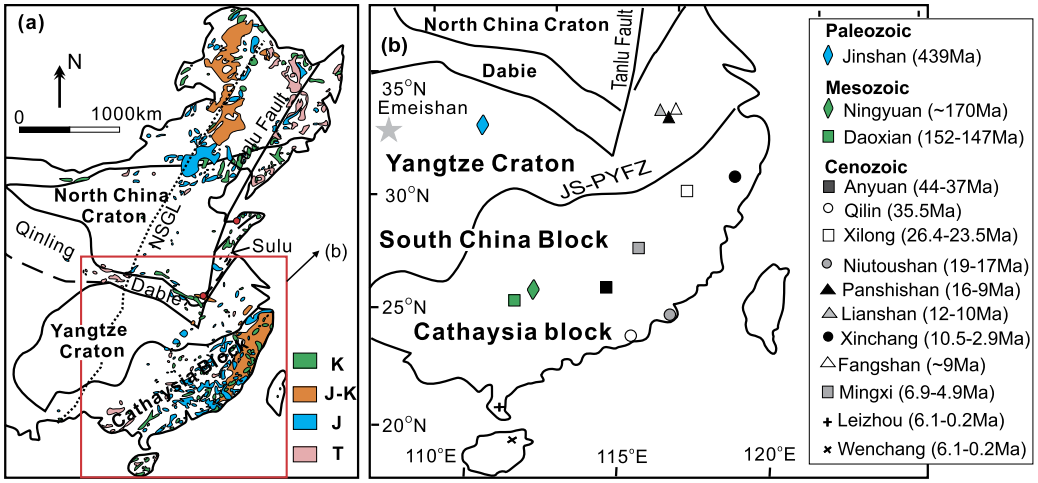

Fig. 1. (a) Map of Phanerozoic magmatic activity in eastern China. (b) Peridotite xenolith localities in the South China Block. Symbols in (a): T, J, J-K and K, is Triassic, Jurassic, Jurassic–Cretaceous (undivided) and Cretaceous, respectively. Uncolored parts represent areas without Phanerozoic magmatic activity. NSGL is the North–South Gravity Lineament, which corresponds to a transition from thick crust and lithosphere with low surface heat flow in the west to thin crust and lithosphere with high surface heat flow in the east. In (b): JS-PYFZ is the Jiangshan–Shaoxing and Pingxiang–Yushan translithospheric fault zone, which represents a Neoproterozoic suture separating the Yangtze Craton from the Cathaysia Block. Symbols are color-coded for age of basalt host: dark blue is Paleozoic, green is Mesozoic, and black, gray and white is Cenozoic. (For interpretation of the references to color in this figure legend, the reader is referred to the web version of this article.)

2. Geological setting and samples

The South China Block is composed of the Yangtze Craton in the north and the Cathaysia block in the south (Fig. 1a), which were amalgamated ~880 Ma ago (Li et al., 2009). Exposed basement in the Yangtze Craton is dominantly Proterozoic with scattered Archean outcrops (Qiu et al., 2000; Zhang et al., 2006). The latter include gneisses with ages of ~2.9 Ga and metasedimentary rocks with zircons of 3.2–2.9 Ga (Qiu et al., 2000). Xenocrystic zircons from Paleozoic lamproite and kimberlite diatremes have U–Pb age peaks of 2.9–2.8 and 2.6–2.5 Ga and peaks of Hf depleted-mantle model ages at 3.5–2.6 Ga (Zheng et al., 2006). These observations suggest that the Yangtze Craton represents Archean basement that was reworked in the Proterozoic, most likely during the amalgamation of micro-continents (Zhao and Cawood, 2012). Cathaysia is composed mainly of Neoproterozoic crust with scattered exposures of Paleoproterozoic basement rocks (Zhao and Cawood, 2012). U–Pb ages and Hf-isotope systematics of xenocrystic zircons within the 166 Ma Pingle minettes and the 48–49 Ma Xiaoliudian and Shuangtian (Fig. 1b) basalts are Archean, showing that highly evolved Archean basement may underlie the block (Zheng et al., 2011).

By the late Triassic, the South China Block appears to have amalgamated with the North China Craton along a suture represented by the Dabie–Sulu UHP belt. Both the North China Craton and the South China Block are small relative to many other cratons, and have been disturbed by post-Archean magmatic events and lithosphere thinning. In the Permian, the Emeishan flood basalts (Fig. 1b) were erupted in the western part of the Yangtze Craton (Chung and Jahn, 1995; Xu et al., 2004). In the Jurassic and Cretaceous, much of eastern China was intruded by granitic plutons, associated with a continental arc developed along the western Pacific subduction system (Fig. 1a). Continental-arc magmatism terminated in the Cenozoic, most likely due to the rollback of the western Pacific subduction zones. This rollback left a broad wake of lithospheric extension in southeastern China, as exemplified by the opening of the South China Sea and other early Tertiary basins (Chung et al., 1994).

One consequence of the Mesozoic–Cenozoic Pacific subduction system was the widespread generation of small-volume intra-plate basaltic volcanism, starting with Jurassic to Cretaceous basalts in the central part of Cathaysia Block followed by Cenozoic basalts scattered throughout the southern and eastern parts (Fig. 1b). Many of these basalts contain mantle xenoliths, providing a window into the deep lithosphere. The xenoliths range from lherzolites (dominant) to harzburgites, mostly in the spinel facies and with minor garnet peridotites (DR Table 1). Pyroxenites are rare in the studied area, although some authors suggested that refertilization may form pyroxenite layers during magmatic underplating at the Moho (e.g., Bodinier et al., 2008) and generate iron-rich garnet-bearing lithologies (e.g., eclogite) at depth.

3. Analytical methods

The data for ~300 samples presented here combine new measurements with data compiled from the literature. Sources of compiled data are given in DR Tables 2–5. For our data, whole-rock major elements were determined by X-ray fluorescence (XRF), mineral major elements were determined by electron microprobe (EPMA), and mineral trace elements were determined by laser-ablation inductively coupled plasma mass spectrometry (LA-ICPMS). Analyses were conducted at the State Key Laboratory of Geological Processes and Mineral Resources, China University of Geosciences (Wuhan). More details of analytical methods can be found in the Data Repository.

4. Results and discussions

Temperatures based on Ca in orthopyroxene coexisting with clinopyroxene, which yields similar results to two-pyroxene thermometer, range from 750 to 1200 °C (DR Tables 2–5). Because of the lack of suitable barometers for spinel peridotites, equilibration pressures could not be calculated for these samples. Pressures could only be calculated on the scarce garnet peridotites found in Cenozoic host basalts at four Cathaysian xenolith localities. Thermobarometric constraints based on garnet-orthopyroxene and two-pyroxene pairs (Brey and Kohler, 2000) record equilibration between 1.8–2.5 GPa and 1100–1250 °C. The average pressure (2.15 GPa) is similar to the estimates (mean 2.20 GPa) for garnet peridotites (Foley et al., 2006). Importantly, the P–T constraints on each suite of garnet peridotites overlap and therefore define a common geotherm, which constrains the thickness of the Cathaysian lithosphere when the basalts erupted, as approximated by the intersection with the mantle adiabat, to be ~100 km

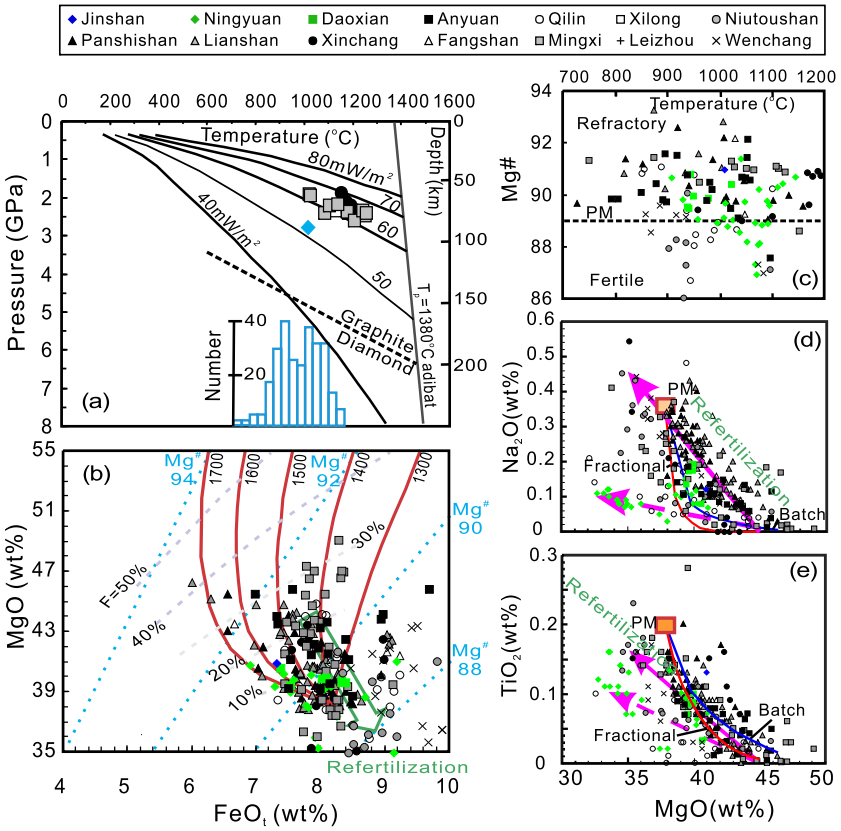

Fig. 2. Xenolith systematics showing (a) thermobarometrically-determined pressure *vs* temperature, (b) whole rock MgO *vs* FeO, where FeO represents all Fe as FeO, (c) whole rock Mg# *vs* temperature, where Mg# = atomic Mg/(Mg + Fe) × 100, (d) and (e) whole rock Na_2O and TiO_2 *vs* MgO respectively. In (a), model steady-state conductive geotherms are pinned to a given surface heat flux ($mW\,m^{-2}$) and crustal heat production taken from Rudnick et al. (1998). Near-vertical line corresponds to a mantle adiabat pinned to a mantle potential temperature T_P of ~1380 °C (Lee et al., 2009). Samples for which we have only temperature constraints are shown as a histogram at the bottom of the panel. In (b), red solid lines represent isothermal melting curves (which approximate adiabatic decompression) taken from Lee et al. (2011) following the approach in Langmuir and Hanson (1981). Gray dashed lines represent melting-degree (F) contours. Blue diagonal lines are contours of constant Mg#. Refertilization is shown by the green arrow and points toward a decrease in Mg#. In (c) to (e), PM represents primitive mantle (McDonough and Sun, 1995). In (d) and (e) blue and orange curves respectively show batch and fractional melting; purple arrows represent refertilization by melt with high Na_2O and TiO_2 contents (solid line) and low Na_2O and TiO_2 contents (dashed line), derived from the mixing between the refractory peridotite (Elthon, 1992) and basaltic melts with 1.6 wt% Na_2O (0.5 wt% TiO_2) and 0.3 wt% Na_2O (0.3 wt% TiO_2), respectively. (For interpretation of the references to color in this figure legend, the reader is referred to the web version of this article.)

(Fig. 2a). The geotherm resembles a model steady-state conductive geotherm corresponding to a surface heat flux of ~60–70 mW/m^2 (also see Xu et al., 1996); this is similar to geotherms calculated for actively extending continental regions, such as the Basin and Range in western USA, and much hotter and thinner than those of typical cratons (~40 mW/m^2 and >200 km) (Pollack et al., 1993). This thin lithosphere is consistent with recent body-wave tomographic studies beneath the South China Block, which show high-velocity anomalies extending to depths of only ~100 km (Huang and Zhao, 2006; Li and van der Hilst, 2010).

To address whether such destabilization may have been driven by compositional changes, which in turn modify density, we mapped the compositional structure of the craton as a function of temperature, which we use as a qualitative proxy for relative depth. There is considerable variation in MgO and FeO (Fig. 2b), manifested as variations in Mg# (atomic Mg/(Mg + Fe) × 100), which increases with increasing melt extraction due to preferential removal of Fe into the melt and retention of Mg in the residue (Fig. 2c). Mg# varies from ultra-fertile values (<87) up to highly melt-depleted values (93). Much of the total range in Mg# is seen at each given temperature, indicating compositional heterogeneity at every level within the continental mantle. Also noteworthy is that the upper envelope Mg# does not vary significantly with temperature, but the lower envelope shows a subtle negative correlation with temperature, suggesting weak tendency to greater fertility with depth.

While the ultra-fertile Mg# are considerably lower than estimates for the modern fertile upper mantle (~89) (McDonough and Sun, 1995), the Mg#s ranging up to 93 are peculiar because such high degrees of melt depletion are virtually non-existent in Phanerozoic peridotites, presumably because mantle potential temperatures during the Phanerozoic were not hot enough (Lee et al., 2011). Such high Mg#s are almost exclusively found in Archean cratonic mantle (Boyd and Mertzman, 1987; Griffin et al., 1999, 2009; Zheng et al., 2001, 2007; Lee et al., 2009) and undoubtedly reflect the higher extents of melting involved in the formation of Archean cratonic mantle protoliths compared to the Phanerozoic. The low FeO contents of the high-Mg# South China Block xenoliths also are typical of Archean lithospheric mantle (Fig. 2b) and require temperatures of melting in excess of 1600 °C, much higher than the potential temperature of Phanerozoic mantle (~1350–1400 °C) (Lee et al., 2009). The highest Mg# peridotites from the South China Block are likely to represent original cratonic mantle, and yet, as a whole, the overall thermal and compositional structure of the South China Block lithosphere does not look cratonic. Why does the South China Block not fit the standard view of cratons?

The presence of ultra-fertile peridotites, the high variability in Mg# at a given depth, and the overall decrease in Mg# with depth (Fig. 2c) suggest that silicate melts have infiltrated into originally depleted cratonic mantle, making it more fertile by melt-rock reaction or impregnation (e.g., refertilization). Additional evidence for melt infiltration is seen in the many xenoliths that

have whole-rock FeO contents higher than the convecting mantle (Fig. 2b). In addition, plots of MgO *vs* FeO_t (Fig. 2b), and incompatible elements like Na (Fig. 2d) and Ti (Fig. 2e) *vs* Mg do not plot on melt-depletion curves, which should be strongly hyperbolic; instead, they plot on linear or scattered arrays, which are most easily explained by mixing processes like refertilization (Elthon, 1992; Le Roux et al., 2007). On the other hand, the presence of a group of samples with intermediate Mg# values and equilibrium temperatures around 900–1000 °C, which show correlations between temperature and metasomatic enrichment (including iron), suggests the possible existence of small-scale temperature gradients in the wall rocks of melt conduits (e.g., Bodinier et al., 2008).

Studies of orogenic peridotites show that refertilization marked by modal enrichments are associated with chemical enrichments in Al, Ca, Na, Ti as well as decreasing Mg# values (e.g., Beyer et al., 2006; Le Roux et al., 2007). However, Mg# generally does not decrease much below 89 in the case of diffuse refertilization, due to efficient buffering of the melts by olivine, and Fe remains roughly constant in whole rocks as the Mg# decrease tends to be balanced by a decrease in olivine proportion (Bodinier et al., 1990). The massifs nevertheless show two cases where Mg# may decrease well below 89 as a result of melt-rock interactions in a broad sense, selective Fe (±Ti) enrichment in wall-rock of melt conduits (typically <25 cm, Bodinier et al., 1990). Fe enrichment may be extreme and is not coupled with modal refertilization, except for subtle "stealth metasomatism" (O'Reilly and Griffin, 2012), nor with Al, Ca and Na enrichment. This process has been recognized as a special form of metasomatism (Fe–Ti metasometism, Menzies and Hawkesworth, 1987) and ascribed to processes that are specific to wall rocks of vein conduits and likely involve melt differentiation in conduits and diffusive Mg–Fe exchange into wall rocks. On the other hand, heterogeneous (veined) refertilization forming pyroxenite layers with a decrease in Mg# (<89) is favoured by a strong decrease in olivine proportion and high melt/rock ratios in high permeability channels (Bodinier et al., 2008). The heterogeneous refertilization can result in very low Mg# ratios (down to 85 or even less) but differs from the Fe–Ti metasomatism because the Mg# variation is coupled with substantial modal changes; rocks with Mg# ~85 are virtually devoid of olivine (Bodinier et al., 2008).

Xenolith studies generally confirm the existence of these two processes, with a range of intermediate situations; for example, low-Mg# rocks are found in suites where igneous cumulate/segregates are abundant, suggesting that they represent the host rocks of igneous intrusions (Ionov et al., 2005), or they are strongly reacted and interpreted as high-permeability channels (Raffone et al., 2009). Compositionally, the subcontinental lithosphere mantle beneath the South China Block is similar to unusually fertile lithospheric mantle beneath the Paleoproterozoic Aldan shield on the margin of the Siberian craton, which has also been interpreted to be the product of refertilization (Ionov et al., 2005). Exactly when such refertilization or refertilization events occurred is unknown. However, the widespread occurrence of Mesozoic plutons throughout southeastern China (see Fig. 1a) indicates that heat and magmas were advected into the crust, which in turn suggests that mantle-derived magmas may have traversed the continental lithosphere, providing at least one window of opportunity for refertilization.

We consider now the effect of refertilization on density. Using empirical parameterizations of density as a function of Mg#, $\rho = -0.0144\text{Mg\#} + 4.66$, where ρ is in g/cm^3 (Lee, 2003), the buoyancy of the South China Block mantle is determined by the density difference between the cratonic mantle and that of the ambient mantle, which we assume to be vigorously convecting and hence, characterized by an adiabatic temperature profile corresponding to a specified mantle potential temperature T_P. This density difference is given by

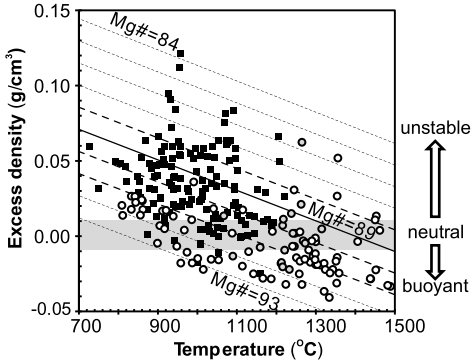

Fig. 3. Density anomaly versus temperature for peridotites from the South China Block. Calculations as described in the text. These anomalies represent densities calculated relative to a primitive mantle reference (Mg# = 89) and a potential temperature of 1380 °C, using parameterizations of Lee (2003). Diagonal lines correspond to densities at constant Mg#. Horizontal zone at zero corresponds to neutral density. Black squares represent peridotite xenoliths from the South China Block in this study. Circles represent densities of xenoliths from stable Archean (white; Slave, South Africa, Tanzania, Siberia) and Proterozoic (gray; Colorado Plateau) cratons from compilations in Lee et al. (2011).

$$\Delta\rho_c = \rho_c(\text{Mg\#}, T_P)\left[1 - \alpha(T_c - T_P)\right] - \rho_o(T_P) \quad (1)$$

where ρ_c (Mg#, T_P) is the density of a continental peridotite at T_P, ρ_o is the density of the ambient convecting mantle at T_P, α is thermal expansivity (3×10^{-5} °C^{-1}), and T_c is the continental peridotite's temperature. We take T_P to equal 1380 °C (Ionov et al., 2005) and reference density of the convecting upper mantle to correspond to Mg# = 89 (Lee et al., 2009), under the assumption that Mg# varies without mineralogical changes. When $\Delta\rho_c = 0$, the low temperatures of the cratonic peridotites are compensated by compositional buoyancy and the continent is neutrally buoyant. In Fig. 3, $\Delta\rho_c$ is plotted against temperature – a proxy for depth – in the continental mantle.

Overall, peridotites from stable Archean cratons have, on average, zero net density anomalies because the compositional and temperature effects are compensatory (Lee, 2003). By contrast, most of peridotites from the South China Block show net positive density anomalies in excess of 0.05 g/cm^3 (or ~1.5%) due to their fertile compositions compared to ambient convecting mantle. These density excesses render the lithospheric mantle beneath the South China Block convectively unstable. The growth time of a convective instability is exponential with order-of-magnitude e-fold growth time scaling as $\eta(\Delta\rho g H)^{-1}$, where η is viscosity, g is gravity, and H is the thickness of the denser layer (Conrad and Molnar, 1997). For a layer 10 km thick with a density excess of 0.05 g/cm^3 (~1.5%) and a viscosity of 10^{21} to 10^{22} Pa s, convective removal of this instability should have occurred within ~10–100 My. Thus, the density structure of the South China Block is likely to be a transient feature, from which it follows that destabilization of these ultra-fertile domains must be happening now or recently (i.e., Phanerozoic), implying that refertilization itself may be an ongoing feature. The lack of Archean Re–Os isotopic model ages in mantle xenoliths from the South China Block (Fig. 4) is consistent with subsequent reworking of the mantle.

To decrease the Mg# of a melt-depleted peridotite from >91 to <86, as seen in the subcontinental lithospheric mantle of the South China Block, large amounts of melt infiltration are required (Ionov et al., 2005), meaning that conditions beneath the lithosphere must have been favorable for melt generation at some point in time. The main factor controlling magma generation beneath a continent is the potential temperature of the mantle and the amount of "headspace" available for decompression melting. This

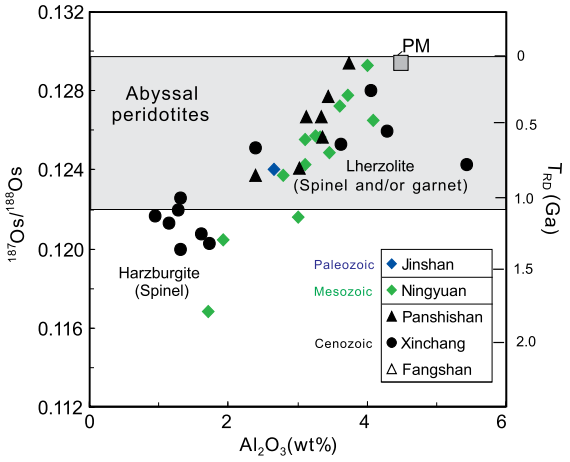

Fig. 4. Plots of $^{187}Os/^{188}Os$ *vs* Al_2O_3 of peridotites from the South China Block. Data sources can be found in DR Table 4. PM, primitive mantle (as in Figs. 2c to 2e).

"headspace" is bounded at its base by the depth at which the mantle adiabat crosses the solidus (which depends on T_P) and at its top by the thickness of the lithosphere (Langmuir et al., 1992; Lee and Chin, 2014). Significant melting only occurs if the lithosphere is thinner than the initial depth of volatile-free melting (volatiles increase initial melting depth but generate only small amounts of additional melt). For a modern T_P of ~1350–1400 °C and allowing for 200 °C of lateral variability to account for plumes and small-scale convective instabilities, it can be seen that only lithospheres thinner than ~150 km can ever be modified by refertilization (Fig. 5). Thicker cratonic lithosphere can be split first and then affected by refertilization as documented for the Labrador Sea (Tappe et al., 2007; Foley, 2008).

For higher average T_P, such as 1600 °C, which may have been more applicable to the Archean, lithospheres would have to be less than 230 km thick to be affected. That is, the critical thickness may evolve with secular cooling of the Earth. In any case, refertilization, once initiated, could destabilize the base of the continental lithosphere, generating more "headspace", which in turn promotes more melting below and hence more potential for refertilization. This positive feedback could lead to eventual destruction. We speculate that the South China Block may be an example of a relatively thin (i.e. initially <230 km), and hence ill-fated, continent. By contrast, boundary layers initially thicker than the average global melting depth should suppress melt generation and hence be relatively immune to refertilization. Lithospheres born thick are thus usually, although not necessarily forever (cf. O'Reilly et al., 2001). The rejuvenation of cratons, dislodging of blocks (Foley, 2008) or formation of metacratons (Liegeois et al., 2013) may result in melt infiltration and refertilization.

5. Conclusions

Although compositional buoyancy plays an important role in stabilizing continents, this is not sufficient to preserve a craton if the compositional buoyancy can be destroyed by refertilization. We suggest that the long-term fate of continents ultimately depends on their initial thickness, which modulates the extent of refertilization-driven destabilization. Other processes, such as hydration-induced weakening or viscous stresses associated with proximity to subduction zones could further enhance destabilization, so relatively small and initially thin cratons would be even more prone to destabilization, as might have been the case for both the North China Craton and the South China Block. Understanding what dictates the structure of continents throughout Earth's history is thus a key to their evolution. If our proposal is correct, long-lived continents must have been built thicker than the maximum depth of ambient melting at the time of their formation (i.e., >250 km). If so, rapid tectonic thickening processes, including mantle overturns, might be necessary to form stable cratons (Cooper et al., 2006; Griffin et al., 2009) as such thickening could depress the base of the lithosphere to below the depth of melt generation.

Acknowledgements

We thank the journal editor (Dr. Y. Ricard) and reviewers (Drs. J.L. Bodinier and S. Foley) for constructive comments and sugges-

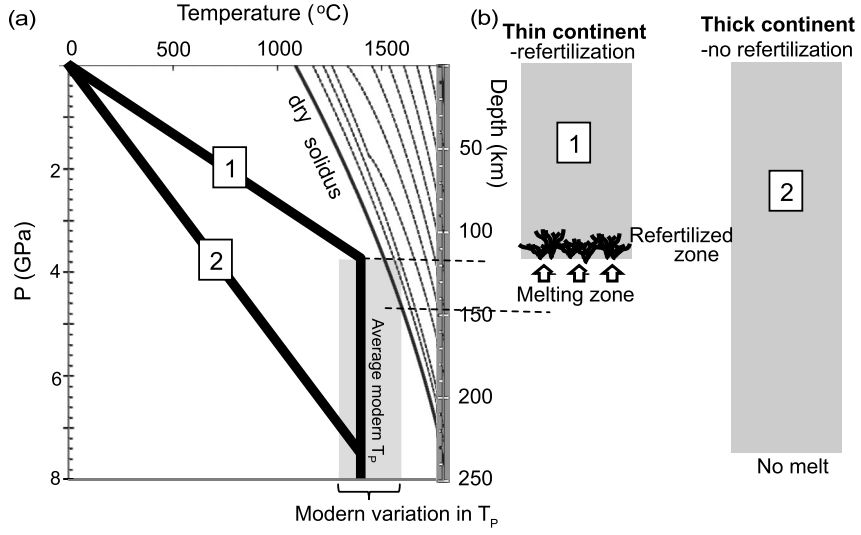

Fig. 5. Cartoon illustrating the concept of refertilization. (a) Pressure (depth) – temperature diagram showing the conditions favorable for generating melts beneath continents. Curved solid line corresponds to the volatile-free solidus of peridotite along with 10% melting-degree contours. Curved dashed line corresponds to water-saturated solidus. Thick diagonal black lines correspond to highly schematized geotherms for a thin (1) and a thick (2) continental lithosphere. Base of lithosphere defined by the intersection of the geotherm with mantle adiabat pinned to average mantle potential temperature, taken here to be 1380 °C. Gray shaded region corresponds to temperature variation in the uppermost mantle away from subduction zones, to account for the effect of thermal plumes and small-scale convective instabilities that may interact with the base of the continent. Melting only occurs where the geotherm of the continental lithosphere or underlying convecting mantle intersects the solidus. (b) Beneath thin lithosphere (and thus small continents), there is sufficient headspace to generate melts, which then rise to fertilize the lithospheric mantle. In contrast, there is insufficient headspace for melting beneath thick (i.e. >250 km) lithosphere, which is minimally affected by refertilization.

tions, and Drs. W.L. Griffin, J. Lassiter and S.A. Gibson for helpful discussions. The study was supported by the NSFC (41130315 and 91214204) and China Geological Survey (Nos. 12120114054201, 12120114016801).

Appendix A. Supplementary material

Supplementary material related to this article can be found online at http://dx.doi.org/10.1016/j.epsl.2014.10.042.

References

Beyer, E.E., Griffin, W.L., O'Reilly, S.Y., 2006. Transformation of Archean lithospheric mantle by refertilisation: evidence from exposed peridotites in the Western Gneiss Region, Norway. J. Petrol. 47, 1611–1636.

Bodinier, J.-L., Vasseur, G., Vernières, J., Dupuy, C., Fabriès, J., 1990. Mechanism of mantle metasomatism: geochemical evidence from the Lherz orogenic peridotite. J. Petrol. 1, 597–628.

Bodinier, J.-L., Garrido, C.J., Chanefo, I., Bruguier, O., Gervilla, F., 2008. Origin of pyroxenite–peridotite veined mantle by refertilization reactions: evidence from the Ronda Peridotite (Southern Spain). J. Petrol. 49, 999–1025.

Boyd, F.R., Mertman, S.A., 1987. Composition and structure of the Kaapvaal lithosphere, southern Africa. In: Mysen, B.O. (Ed.), Magmatic Processes: Physicochemical Principles. The Geochemical Society, Special Publication 1, 13–24.

Brey, G.P., Kohler, T., 2000. Geothermobarometry in four-phase lherzolites II. New thermobarometers, and practical assessment of existing thermobarometers. J. Petrol. 31, 1353–1378.

Carlson, R.W., Irving, A.J., Schulze, D.J., Hearn Jr., B.C., 2004. Timing of Precambrian melt depletion and Phanerozoic refertilization events in the lithospheric mantle of the Wyoming Craton and adjacent Central Plains Orogen. Lithos 77, 453–472.

Chung, S.-L., Jahn, B.M., 1995. Plume-lithosphere interaction in generation of the Emishan flood basalts at the Permian–Triassic boundary. Geology 23, 889–892.

Chung, S.-L., Sun, S.S., Tu, K., Chen, C.H., Lee, C.Y., 1994. Late Cenozoic basaltic volcanism around the Taiwan strait, southeast China: product of lithosphere–asthenosphere interaction during continental extension. Chem. Geol. 112, 1–20.

Conrad, C.P., Molnar, P., 1997. The growth of Rayleigh–Taylor-type instabilities in the lithosphere for various rheological and density structures. Geophys. J. Int. 129, 95–112.

Cooper, C.M., Lenardic, A., Levander, A., Moresi, L., 2006. Creation and preservation of cratonic lithosphere: seismic constraints and geodynamic models. AGU Monograph 164, 75–88.

Elthon, D., 1992. Chemical trends in abyssal peridotites: refertilization of depleted suboceanic mantle. J. Geophys. Res. 97, 9015–9025.

Foley, S.F., 2008. Rejuvenation and erosion of the cratonic lithosphere. Nat. Geosci. 1, 503–510.

Foley, S.F., Andronikov, A.V., Jacob, D.E., Melzer, S., 2006. Evidence from Antarctic mantle peridotite xenoliths for changes in mineralogy, geochemistry and geothermal gradients beneath a developing rift. Geochim. Cosmochim. Acta 70, 3096–3120.

Griffin, W.L., O'Reilly, S.Y., Ryan, C.G., 1999. The composition and origin of subcontinental lithospheric mantle. In: Fei, Y., Berka, C.M., Mysen, B.O. (Eds.), Mantle Petrology: Field Observations and High-pressure Experimentation: A Tribute to Francis R. (Joe) Boyd. In: The Geochemical Society, Special Publication, vol. 6, pp. 13–45.

Griffin, W.L., O'Reilly, S.Y., Afonso, J.C., Begg, G., 2009. The composition and evolution of lithospheric mantle: a re-evaluation and its tectonic implications. J. Petrol. 50, 1185–1204.

Herzberg, C., Rudnick, R.L., 2012. Formation of cratonic lithosphere: an integrated thermal and petrological model. Lithos. http://dx.doi.org/10.1016/j.lithos.2012.01.010.

Huang, J., Zhao, D., 2006. High-resolution mantle tomography of China and surrounding regions. J. Geophys. Res. 111 (B9), 305. http://dx.doi.org/10.1029/2005JB004066.

Hughes, H.S.R., McDonald, I., Goodenough, Kathryn M., Ciborowski, T.J.R., Kerr, A.C., Davies, J., Selby, D., 2014. Enriched lithospheric mantle keel below the Scottish margin of the North Atlantic Craton: evidence from the Palaeoproterozoic Scourie Dyke Swarm and mantle xenoliths. Precambrian Res. 250, 97–126.

Ionov, D.A., Chanefo, I., Bodinier, J.L., 2005. Origin of Fe-rich lherzolites and wehrlites from Tok, SE Siberia by reactive melt percolation in refractory mantle peridotites. Contrib. Mineral. Petrol. 150, 335–353.

Jordan, T.H., 1978. Composition and development of the continental tectosphere. Nature 274, 544–548.

Kelly, R.K., Kelemen, P.B., Jull, M., 2003. Buoyancy of the continental upper mantle. Geochem. Geophys. Geosyst. 4, 1017.

Kusky, T.M., Windley, B.F., Wang, L., Wang, Z.S., Li, X.Y., Zhu, P.M., 2014. Flat slab subduction, trench suction, and craton destruction: comparison of the North China, Wyoming, and Brazilian cratons. Tectonophysics 630, 208–221.

Langmuir, C.H., Hanson, G.N., 1981. In: Newton, R.C., Navrotsky, A., Wood, B.J. (Eds.), Thermodynamics of Minerals and Melts. Springer, pp. 247–271.

Langmuir, C., Klein, E.M., Plank, T., 1992. Geophys. Monogr., vol. 71. American Geophysical Union, pp. 183–280.

Le Roux, V., Bodinier, J.-L., Tommasi, A., Alard, O., Dautria, J.M., Vauchez, A., Riches, A.J.V., 2007. The Lherz spinel lherzolite: refertilized rather than pristine mantle. Earth Planet. Sci. Lett. 259, 599–612.

Lee, C.-T.A., 2003. Compositional variation of density and seismic velocities in natural peridotites at STP conditions: implications for seismic imaging of compositional heterogeneities in the upper mantle. J. Geophys. Res. 108. http://dx.doi.org/10.1029/2003JB002413.

Lee, C.-T.A., Chin, E.J., 2014. Calculating melting temperatures and pressures of peridotite protoliths: implications for the origin of cratonic mantle. Earth Planet. Sci. Lett. 403, 273–286.

Lee, C.-T.A., Luffi, P., Plank, T., Dalton, H.A., Leeman, W.P., 2009. Constraints on the depths and temperatures of basaltic magma generation on Earth and other terrestrial planets using new thermobarometers for mafic magmas. Earth Planet. Sci. Lett. 279, 20–33.

Lee, C.-T.A., Luffi, P., Chin, E.J., 2011. Building and destroying continental mantle. Annu. Rev. Earth Planet. Sci. 39, 59–90.

Li, C., van der Hilst, R., 2010. Structure of the upper mantle and transition zone beneath Southeast Asia from traveltime tomography. J. Geophys. Res. 115 (B7), 308. http://dx.doi.org/10.1029/2009JB006882.

Li, X.-H., Li, W.X., Li, Z.X., 2009. Amalgamation between the Yangtze and Cathaysia blocks in south China: constraints from SHRIMP U–Pb zircon ages, geochemistry and Nd–Hf isotopes of the Shuangxiwu volcanic rocks. Precambrian Res. 174, 117–128.

Liegeois, J.P., Abdelsalam, M.G., Ennih, N., Ouabadi, A., 2013. Metacraton: nature, genesis and behavior. Gondwana Res. 23, 220–237.

Liu, C.Z., Liu, Z.C., Wu, F.Y., Chu, Z.Y., 2012a. Mesozoic accretion of juvenile subcontinental lithospheric mantle beneath South China and its implications: geochemical and Re–Os isotopic results from Ningyuan mantle xenoliths. Chem. Geol. 291, 186–198.

Liu, C.Z., Wu, F.Y., Sun, J., Chu, Z.Y., Qiu, Z.L., 2012b. The Xinchang peridotite xenoliths reveal mantle replacement and accretion in southeastern China. Lithos 150, 171–187.

Lu, J.G., Zheng, J.P., Griffin, W.L., Yu, C.M., 2013. Petrology and geochemistry of peridotite xenoliths from the Lianshan region: nature and evolution of lithospheric mantle beneath the lower Yangtze block. Gondwana Res. 23, 161–175.

McDonough, W.F., Sun, S.-S., 1995. The composition of the Earth. Chem. Geol. 120, 223–253.

Menzies, M.A., Hawkesworth, C.J., 1987. Mantle Metasomatism. Academic Press, London, p. 472.

O'Reilly, S.Y., Griffin, W.L., 2012. Mantle metasomatism. In: Harlov, D.E., Austrheim, H. (Eds.), Metasomatism and the Chemical Transformation of Rock. In: Lecture Notes in Earth System Sciences. Springer-Verlag, Berlin, Heidelberg, pp. 467–528.

O'Reilly, S.Y., Griffin, W.L., Poudjom Djomani, Y., Morgan, P., 2001. Are lithospheres forever? Tracking changes in subcontinental lithospheric mantle through time. GSA Today 11, 4–9.

Pollack, H.N., Hurter, S.J., Johnson, J.R., 1993. Heat flow from the Earth's interior; analysis of the global data set. Rev. Geophys. 31, 267–280.

Qiu, Y.M., Gao, S., McNaugton, N.J., Groves, D.I., Ling, W.L., 2000. First evidence of >3.2 Ga continental crust in the Yangtze craton of south China and its implications for Archean crustal evolution and Phanerozoic tectonics. Geology 28, 11–14.

Raffone, N., Chazot, G., Pin, C., Vanucci, R., Zanetti, A., 2009. Metasomatism in the lithospheric mantle beneath Middle Atlas (Morocco) and the origin of Fe- and Mg-rich wehrlites. J. Petrol. 50, 197–249.

Rudnick, R.L., McDonough, W.F., O'Connell, R.J., 1998. Thermal structure, thickness and composition of continental lithosphere. Chem. Geol. 145, 395–411.

Tappe, S., Foley, S.F., Stracke, A., Romer, R.L., Kjarsgaard, B.A., Heaman, L.M., Joyce, 2007. Craton reactivation on the Labrador Sea margins: $^{40}Ar/^{39}Ar$ age and Sr–Nd–Hf–Pb isotope constraints from alkaline and carbonatite intrusives. Earth Planet. Sci. Lett. 256, 433–454.

Wittig, N., Webb, M., Pearson, D.G., Dale, C.W., Ottley, C.J., Hutchison, M., Jensen, S.M., Luguet, A., 2010. Formation of the North Atlantic Craton: timing and mechanisms constrained from Re–Os isotope and PGE data of peridotite xenoliths from S.W. Greenland. Chem. Geol. 276, 166–187.

Xu, X.S., O'Reilly, S.Y., Zhou, X.M., Griffin, W.L., 1996. A xenolith-derived geotherm and the crust–mantle boundary at Qilin, southeastern China. Lithos 38, 41–62.

Xu, X.S., O'Reilly, S.Y., Griffin, W.L., Zhou, X., 1998. The nature of the Cenozoic lithosphere at Nushan, eastern China. In: Flower, M., Chung, S.L., Lo, C.H. (Eds.), Mantle Dynamics and Plate Internationals in East Asia. In: Am. Geophys. Union Geodyn. Ser., vol. 27, pp. 167–196.

Xu, Y.G., Sun, M., Yan, W., Liu, Y., Huang, X.L., Chen, X.M., 2002. Xenolith evidence for polybaric melting and stratification of the upper mantle beneath South China. J. Asian Earth Sci. 20, 937–954.

Xu, Y.G., He, B., Chung, S.-L., Menzies, M., Frey, F.A., 2004. Geologic, geochemical, and geophysical consequences of plume involvement in the Emishan flood-basalt province. Geology 32, 917–920.

Zhang, S.B., Zheng, Y.F., Wu, Y.B., 2006. Zircon isotope evidence for >3.5 Ga continental crust in the Yangtze craton of China. Precambrian Res. 146, 16–34.
Zhao, G.C., Cawood, P.A., 2012. Precambrian geology of China. Precambrian Res. 222–223, 13–54.
Zheng, J.P., O'Reilly, S.Y., Griffin, W.L., Lu, F.X., Zhang, M., 2001. Relics of the Archean mantle beneath eastern part of the North China block and its significance in lithospheric evolution. Lithos 57, 43–66.
Zheng, J.P., O'Reilly, S.Y., Griffin, W.L., Zhang, M., Lu, F.X., Liu, G.L., 2004. Nature and evolution of Mesozoic–Cenozoic lithospheric mantle beneath the Cathaysia block, SE China. Lithos 74, 41–65.
Zheng, J.P., Griffin, W.L., O'Reilly, S.Y., Zhang, M., Pearson, N., 2006. Widespread Archean basement beneath the Yangtze craton. Geology 34, 417–420.
Zheng, J.P., Griffin, W.L., O'Reilly, S.Y., Yu, C.M., Zhang, H.F., Pearson, N., Zhang, M., 2007. Mechanism and timing of lithospheric modification and replacement beneath the eastern North China Craton: peridotitic xenoliths from the 100 Ma Fuxin basalts and a regional synthesis. Geochim. Cosmochim. Acta 71, 5203–5225.
Zheng, J.P., Griffin, W.L., Li, R.S., 2011. Highly evolved Archean basement beneath the western Cathaysia block, south China. Geochim. Cosmochim. Acta 75, 242–255.